



J. Serb. Chem. Soc. 76 (9) 1237–1246 (2011)
JSCS–4200

Synthesis, spectral, thermal and biological studies of transition metal complexes of 4-hydroxy-3-[3-(4-hydroxyphenyl)-acryloyl]-6-methyl-2H-pyran-2-one

VAIBHAV N. PATANGE^{1*} and BALASAHEB R. ARBAD²

¹Department of Chemistry, Research and P. G. Center, Shri Chhatrapati Shivaji College, Omerga, Dist-Osmanabad-413606, Maharashtra and ²Department of Chemistry, Dr. Babasaheb Ambedkar Marathwada University, Aurangabad-431004, Maharashtra, India

(Received 31 May 2010, revised 4 March 2011)

Abstract: The solid complexes of Mn(II), Fe(III), Co(II), Ni(II), and Cu(II) with 4-hydroxy-3-[(2*E*)-3-(4-hydroxyphenyl)prop-2-enoyl]-6-methyl-2*H*-pyran-2-one, derived from 3-acetyl-6-methyl-2*H*-pyran-2,4(3*H*)-dione (dehydroacetic acid) and 4-hydroxybenzaldehyde, were synthesized and characterized by elemental analysis, conductometry, thermal analysis, magnetic measurements, IR, ¹H-NMR and UV–Vis spectroscopy and a biological study. From the analytical and spectral data, the stoichiometry of the complexes was found to be 1:2 (metal:ligand). The physico–chemical data suggest a distorted octahedral geometry for the Cu(II) complexes and an octahedral geometry for all the other complexes. The thermal decomposition of all the complexes was studied by the TG–DTA method. The synthesized ligand and its metal complexes were screened for their *in vitro* antibacterial activity against Gram-negative (*Escherichia coli*) and Gram-positive (*Staphylococcus aureus*) bacterial strains and for *in vitro* antifungal activity against *Aspergillus flavus*, *Curvularia lunata* and *Penicillium notatum*. The results of these studies showed the metal complexes to be more antibacterial/antifungal against one or more species as compared with the non-complexed ligand.

Keywords: dehydroacetic acid; biological activity; transition metal complexes.

INTRODUCTION

The multifarious role of transition metal complexes in biochemistry has been directing the development of new chemistry with metal ligand systems. This has stimulated enormous interest in the synthesis of transition metal complexes with oxygen and nitrogen donor groups, due to the wide range of pharmacological activities of such compounds. In recent years, there has been a growing interest in compounds containing a carbonyl group directly linked to an α,β -unsaturated system (chalcones) and their presumed role in the prevention of various degene-

*Corresponding author. E-mail: drvnpcchem@yahoo.in
doi: 10.2298/JSC100531108P

rative diseases. Chalcones are important compounds because of their contribution to human health and their multiple biological effects.^{1–8} It is believed that the ($>\text{CO}-\text{C}=\text{C}<$), moiety imparts biological characteristics to this class of compounds. Such α,β -unsaturated carbonyl compounds and their metal complexes possess interesting biochemical properties, such as antitumour, antioxidant, antifungal and antimicrobial activities.^{9–15} Therefore, the synthesis and characterisation of such compounds and their metal complexes have tremendous importance. In view of the above facts, it was considered of interest to study the ligation behaviour of such compounds containing α,β -unsaturated linkage(s).^{16–19} The aim of this work was to: *i*) synthesize and characterize the solid complexes of a ligand containing a carbonyl group directly linked to the α,β -unsaturated system derived from 3-acetyl-6-methyl-2*H*-pyran-2,4(3*H*)-dione (dehydroacetic acid) and 4-hydroxybenzaldehyde with Mn(II), Fe(III), Co(II), Ni(II) and Cu(II) and *ii*) to investigate their antibacterial activity towards Gram-positive bacteria (*Staphylococcus aureus*) and Gram-negative bacteria (*Escherichia coli*), and their fungicidal activity towards *Aspergillus flavus*, *Curvularia lunata* and *Penicillium notatum* fungi.

EXPERIMENTAL

The dehydroacetic acid and *p*-hydroxybenzaldehyde used for the preparation of ligand were from Merck and Aldrich, respectively. The metal chlorides used for complex preparation were from BDH. The carbon, hydrogen and nitrogen content in each sample were measured on a Perkin Elmer (2400) CHNS analyzer. The IR spectra (KBr), in the range of 4000–450 cm^{-1} , were recorded on a Perkin Elmer (C-75430) IR spectrometer. The ^1H -NMR spectrum of the ligand was measured in CDCl_3 on a Varian Mercury YH 300 MHz instrument. Atomic absorption spectroscopy (AAS) and thermogravimetric analysis–differential thermal analysis (TGA–DTA) were realised on a Perkin Elmer PE-Analyst 300 and TA/SDT-2960 instruments, respectively. The UV–Vis spectra of the complexes were recorded on a Shimadzu UV-1601 spectrophotometer. Magnetic susceptibility measurements of the complexes were performed using a Gouy balance at room temperature using $\text{Hg}[\text{Co}(\text{SCN})_4]$ as the calibrant. The molar conductivity was measured on an Elico CM180 conductivity meter with a dip-type cell using 10^{-3} M solution of the complexes in dimethylformamide (DMF).

Synthesis of the ligand (HL)

A solution of 0.01 mol of dehydroacetic acid, 10 drops of piperidine and 0.01 mole of *p*-hydroxybenzaldehyde in 25 ml chloroform were refluxed for 8–10 h. 10 ml of the chloroform–water azeotrope mixture was separated by distillation. Crystals of product separated on slow evaporation of the remaining chloroform. The resulting orange precipitate was filtered, washed several times with ethanol and crystallized from chloroform (Fig. 1).

Synthesis of the metal complexes

To a DMF solution (30 ml) of the ligand (10 mmol) was added a DMF solution (20 ml) of a metal chloride (5 mmol) under constant stirring. The mixture was then refluxed for 2 h and poured on ice-cold water. The resulting metal complex was filtered and washed with cold DMF, petroleum-ether and dried over calcium chloride in a vacuum desiccator.

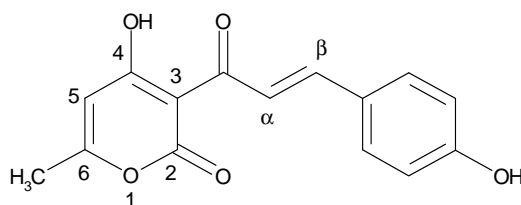


Fig. 1. The proposed structure of the ligand.

Antimicrobial activity

The ligand and its metal complexes were screened for *in vitro* antibacterial activity against Gram-positive bacteria, *i.e.*, *Staphylococcus aureus* and Gram-negative bacteria, *i.e.*, *Escherichia coli* by the paper disc plate method.²⁰ The compounds were tested at concentrations of 0.50 and 1.0 mg ml⁻¹ in DMF (0.1 mL) was placed on a paper disk (6 mm in diameter) with the help of micropipette and compared with a known antibiotic, *viz.* neomycin at the same concentrations. To evaluate the fungicidal activity of the ligands and the metal complexes, their effects on the growth of *Aspergillus flavus*, *Curvularia lunata* and *Penicillium notatum* were studied. The ligand and their corresponding metal chelates in DMF were screened *in vitro* by the disc diffusion method.²¹ The ligands and complexes were dissolved separately in DMF to obtain concentration of 125 and 250 µg disc⁻¹. The linear growth of the fungus was recorded by measuring the diameter of the colony after 96 h. The diameters of the zone of inhibition produced by the complexes were compared with griseofulvin, an antifungal drug.

RESULTS AND DISCUSSION

The elemental analyses showed 1:2 (metal:ligand) stoichiometry for all the complexes (Fig. 2). The analytical data of the ligand and its metal complexes

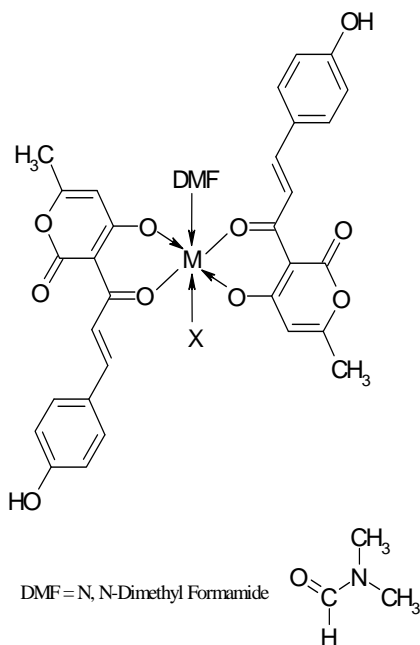


Fig. 2. The proposed structure of the complexes. X = DMF when M = Mn(II), Co(II) Ni(II) and Cu(II), and X = Cl when M = Fe(III).

corresponded well with the general formula $[M(L)_2(DMF)_2]$, where $M = Mn(II)$, $Co(II)$, $Ni(II)$, $Cu(II)$, and $[M(L)_2(DMF)(Cl)]$, where $M = Fe(III)$, $L = C_{15}H_{11}O_5$. The absence of chlorine except in the $Fe(III)$ complex was evident from the Volhard test. The complexes were coloured, stable in air, insoluble in water and common solvents, except for DMF and dimethyl sulphoxide (DMSO). The low conductance of the complexes in DMF solution supported the non-electrolytic nature of the metal complexes (Table I).

TABLE I. Analytical and molar conductance data of the ligand and its metal complexes

Compound	Colour	Found (calcd.) %				FW	Decomposition temperature, °C	A_m $\Omega^{-1} \text{ cm}^2 \text{ mol}^{-1}$
		C	H	N	M			
Ligand, $C_{15}H_{12}O_5$	Orange	63.01 (63.57)	4.67 (4.67)	–	–	272.3	235	–
$[C_{36}H_{36}N_2O_{12}Mn]$	Light brown	58.42 (58.15)	4.86 (4.87)	3.66 (3.76)	7.02 (7.39)	743.6	267	15.1
$[C_{33}H_{29}NO_{11}ClFe]$	Dark brown	56.12 (56.07)	4.33 (4.13)	1.82 (1.92)	7.62 (7.89)	706.9	>300	15.3
$[C_{36}H_{36}N_2O_{12}Co]$	Brown	56.99 (57.84)	4.52 (4.85)	3.83 (3.74)	7.72 (7.88)	747.6	>300	22.7
$[C_{36}H_{36}N_2O_{12}Ni]$	Green	58.01 (57.85)	4.71 (4.85)	3.82 (3.74)	7.63 (7.85)	747.4	>300	9.8
$[C_{36}H_{36}N_2O_{12}Cu]$	Green	57.12 (57.48)	4.21 (4.82)	3.52 (3.72)	8.31 (8.44)	752.2	283	10.5

Infrared spectra

Important spectral bands for the ligand and its metal complexes are presented in Table II. The IR spectrum of the ligand show band at 3256 and 3112 cm^{-1} assignable to $\nu(\text{OH})$ of the intramolecular phenolic group of the dehydroacetic acid moiety and $\nu(\text{OH})$ of aromatic ring, respectively. Other bands at 1697, 1675 and 1223 cm^{-1} are assignable to $\nu(\text{C}=\text{O})$ (lactone carbonyl), $\nu(\text{C}=\text{O})$ (acetyl carbonyl) and $\nu(\text{C}-\text{O})$ (phenolic) stretching mode, respectively.^{22,23} In the IR spectra of all the metal complexes, the broad medium intensity band centred in the region 3500–3200 cm^{-1} corresponds to aromatic $\nu(\text{OH})$. No band was observed in the IR spectra of the metal chelates in the region 3256 cm^{-1} . The absence of $\nu(\text{OH})$ (phenolic) at 3256 cm^{-1} suggests subsequent deprotonation of the phenolic group and coordination of phenolic oxygen to the metal ion. This was supported by an upward shift in $\nu(\text{C}-\text{O})$ (phenolic)²⁴ by 50–60 cm^{-1} . The $\nu(\text{C}=\text{O})$ (acetyl carbonyl) in all the metal complexes was shifted by 40–60 cm^{-1} to a lower energy with respect to that of the free ligand, indicating the participation of $\nu(\text{C}=\text{O})$ (acetyl carbonyl) in the coordination.^{22,23} The IR spectra of all the compounds showed a prominent band at $\approx 970 \text{ cm}^{-1}$, typical of *trans* $-\text{CH}=\text{CH}-$ absorption.²⁵ The presence of new bands in the region 600–450 cm^{-1} can be as-

signed to $\nu(\text{M}-\text{O})$ vibrations.²⁶ According to the above-mentioned data, the ligand behaved as monodeprotonated bidentate and the coordination occurred *via* the acetyl and phenolic oxygen of the dehydroacetic acid moiety, as shown in Fig. 1.

TABLE II. Characteristic IR frequencies (cm^{-1}) of the ligand and its metal complexes

Compound	$\nu(\text{OH})$ (aromatic ring)	$\nu(\text{OH})$ (dehyd- roacetic acid moiety)	$\nu(\text{C}=\text{O})$ (lactone)	$\nu(\text{C}=\text{O})$ (acetyl carbonyl)	$\nu(\text{C}-\text{O})$ (phenolic)	$\nu(\text{C}=\text{C})$ (<i>trans</i>)	$\nu(\text{M}-\text{O})$
Ligand, $\text{C}_{15}\text{H}_{12}\text{O}_5$	3256 (s)	3112 (s)	1697 (m)	1675 (m)	1223 (m)	980 (m)	–
$[\text{C}_{36}\text{H}_{36}\text{N}_2\text{O}_{12}\text{Mn}]$	3251 (s)	–	1678 (m)	1603 (m)	1280 (m)	975 (m)	560 (m) 462 (m)
$[\text{C}_{33}\text{H}_{29}\text{NO}_{11}\text{ClFe}]$	3257 (s)	–	1680 (s)	1621 (m)	1280 (m)	975 (m)	530 (w) 488 (m)
$[\text{C}_{36}\text{H}_{36}\text{N}_2\text{O}_{12}\text{Co}]$	3252 (s)	–	1683 (w)	1620 (m)	1277 (m)	970 (m)	531 (w) 476 (m)
$[\text{C}_{36}\text{H}_{36}\text{N}_2\text{O}_{12}\text{Ni}]$	3256 (s)	–	1680 (w)	1622 (w)	1277 (m)	988 (m)	551 (m) 531 (w)
$[\text{C}_{36}\text{H}_{36}\text{N}_2\text{O}_{12}\text{Cu}]$	3251 (s)	–	1686 (m)	1628 (m)	1280 (m)	967 (m)	560 (w) 480 (m)

¹H-NMR spectrum of the ligand

The ¹H-NMR spectrum of the ligand in CDCl_3 with TMS as an internal standard showed a singlet at 2.27 ppm for the 3 hydrogens of the methyl group attached to C_6 (Fig. 1), a singlet at 5.39 ppm for the one hydrogen of C_5 , a singlet at 6.33 ppm for the one hydrogen of the aromatic OH, a multiplet at 6.8–7.6 ppm for the four hydrogens of the aromatic ring, a doublet at 7.9–8.19 ppm for the two olefinic protons ($J = 14$ Hz) and a singlet at 18.16 ppm for the one hydrogen of C_4 (phenolic hydrogen).

Magnetic moment and UV-Vis Spectra

The electronic spectra of all the complexes were recorded in DMF solution. The electronic spectrum of the Mn(II) complex exhibited three bands at 18345 cm^{-1} ($\epsilon = 26 \text{ dm}^3 \text{ mol}^{-1} \text{ cm}^{-1}$), 19763 cm^{-1} ($\epsilon = 16 \text{ dm}^3 \text{ mol}^{-1} \text{ cm}^{-1}$) and 23154 cm^{-1} ($\epsilon = 28 \text{ dm}^3 \text{ mol}^{-1} \text{ cm}^{-1}$), which are assigned to ${}^6\text{A}_{1g} \rightarrow {}^4\text{T}_{1g}(\text{G})$, ${}^6\text{A}_{1g} \rightarrow {}^4\text{T}_{2g}(\text{G})$ and ${}^6\text{A}_{1g} \rightarrow {}^4\text{A}_{1g}$, ${}^4\text{E}_g(4\text{G})$ transitions, respectively, indicating an octahedral configuration^{27,28} around the Mn(II) ion. The octahedral geometry of Mn(II) was further confirmed by the value of the magnetic moment ($5.84 \mu_B$).

Three electronic transitions were observed in the electronic spectrum of the Fe(III) complex, at 14472 cm^{-1} ($\epsilon = 22 \text{ dm}^3 \text{ mol}^{-1} \text{ cm}^{-1}$), 21322 cm^{-1} ($\epsilon = 26 \text{ dm}^3 \text{ mol}^{-1} \text{ cm}^{-1}$) and 24272 cm^{-1} ($\epsilon = 32 \text{ dm}^3 \text{ mol}^{-1} \text{ cm}^{-1}$), which are assigned to ${}^6\text{A}_{1g} \rightarrow {}^4\text{T}_{1g}(\text{G})$, ${}^6\text{A}_{1g} \rightarrow {}^4\text{T}_{2g}(\text{G})$ and ${}^6\text{A}_{1g} \rightarrow {}^4\text{E}_g(\text{G})$, respectively, sug-

gesting an octahedral complex of Fe(III), which was confirmed by the value of magnetic moment ($5.93 \mu_B$).²⁸

The electronic spectrum of the Co(II) complex exhibited three bands at 9487 cm^{-1} ($\epsilon = 17 \text{ dm}^3 \text{ mol}^{-1} \text{ cm}^{-1}$), 18656 cm^{-1} ($\epsilon = 59 \text{ dm}^3 \text{ mol}^{-1} \text{ cm}^{-1}$) and 21551 cm^{-1} ($\epsilon = 98 \text{ dm}^3 \text{ mol}^{-1} \text{ cm}^{-1}$), which are assigned to ${}^4T_{1g}(F) \rightarrow {}^4T_{2g}(F)$, ${}^4T_{1g}(F) \rightarrow {}^4A_{2g}(F)$ and ${}^4T_{1g}(F) \rightarrow {}^4T_{1g}(P)$, respectively, indicating octahedral configuration around the Co(II) ion. The magnetic moment of the Co(II) complex was $4.54 \mu_B$. The calculated spectral parameters ν_2/ν_1 , $10Dq$, B , β and the ligand field stabilizing energy ($LFSE$) have the values 1.96 , 9169 cm^{-1} , 783.1 cm^{-1} , 0.81 and $26.20 \text{ kcal mol}^{-1}$, respectively, which are in good agreement with the reported values of an octahedral Co(II) complex.²⁸

The electronic spectrum of the Ni(II) complex exhibited three bands at 9345 cm^{-1} ($\epsilon = 34 \text{ dm}^3 \text{ mol}^{-1} \text{ cm}^{-1}$), 15698 cm^{-1} ($\epsilon = 67 \text{ dm}^3 \text{ mol}^{-1} \text{ cm}^{-1}$) and 22471 cm^{-1} ($\epsilon = 188 \text{ dm}^3 \text{ mol}^{-1} \text{ cm}^{-1}$), which are assigned to ${}^3A_{2g} \rightarrow {}^3T_{2g}(F)$, ${}^3A_{2g} \rightarrow {}^3T_{1g}(F)$ and ${}^3A_{2g} \rightarrow {}^3T_{1g}(P)$, respectively. The ligand field parameters ν_2/ν_1 , $10Dq$, B , β and the $LFSE$ have the values 1.68 , 9345 cm^{-1} , 675.6 cm^{-1} , 0.65 and $26.69 \text{ kcal mol}^{-1}$, respectively. These values, as well as the magnetic moment value ($3.13 \mu_B$), support an octahedral geometry of the Ni(II) complex.²⁸

The spectrum of the Cu(II) complex consisted of a broad band at 14225 cm^{-1} ($\epsilon = 94 \text{ dm}^3 \text{ mol}^{-1} \text{ cm}^{-1}$), assigned to the ${}^2E_g \rightarrow {}^2T_{2g}$ transition of a distorted octahedral geometry.²⁹ In addition to this band, the band observed at 25316 cm^{-1} ($\epsilon = 1143 \text{ dm}^3 \text{ mol}^{-1} \text{ cm}^{-1}$) arises from intra ligand charge transfer. The $LFSE$ value of the Cu(II) complex is $42.64 \text{ kcal mol}^{-1}$. The obtained values of $LFSE$ determine the stability of the complexes and follows the order in terms of metal ions $\text{Cu(II)} > \text{Ni(II)} > \text{Co(II)}$.

Thermal analysis

All the complexes showed high thermal stability and decomposed above 250°C , indicating the absence of any lattice or coordinated water molecules. The TG curve of the Mn(II) complex showed a rapid first step decomposition between $240\text{--}350^\circ\text{C}$ with 48% mass loss (calcd. 48.14%), associated with an exothermic peak on the DTA curve ($\Delta T_{\text{max}} = 247.38^\circ\text{C}$), indicating the loss of two coordinated DMF molecules and the non-coordinated part of the complex, *i.e.*, the aromatic ring with a beta carbon.³⁰ The complex did not remain stable at higher temperatures and exhibited a slow second step decomposition in the temperature range $360\text{--}950^\circ\text{C}$ with a mass loss of 42% (calcd. 42.22%). The broad endothermic peak for this step on the DTA curve corresponds to the oxidative degradation of the coordinated part of the ligand. The decomposition was completed at $\approx 950^\circ\text{C}$ leading to the formation of the stable metal oxide MnO (observed 10% , calcd. 9.54%). The thermal study of the Fe(III) complex shows stability up to 325°C . The first step showed a rapid decomposition between $340\text{--}400^\circ\text{C}$ with a 45% mass loss (calcd. 45.3%). A broad exotherm was observed

in the DTA ($\Delta T_{\max} = 366.1$ °C). This step may be attributed to the removal of one coordinated DMF molecule, one chloride ion (may be oxidized as Cl_2) and the non-coordinated part of the ligand. The complex continued slow decomposition of the remaining part of the ligand with a mass loss of 44 % (calcd. 44.42 %) in the temperature range 400–900 °C. A broad endotherm was observed for this step in the DTA. The mass of the final residue corresponds to the stable FeO (observed 11 %, calcd. 10.2 %). The Co(II) complex decomposed in two successive steps in the temperature range of 300–850 °C. Two coordinated DMF molecules and the non-coordinated part of the ligand were removed in the first step at 300–400 °C with a mass loss 47.5 % (calcd. 47.88 %). A broad exothermic peak was observed between 200–400 °C ($\Delta T_{\max} = 338.12$ °C). The complex finally decomposed to CoO with the removal of the coordinated part of the ligand (observed 42 %, calcd. 42 %) in the temperature range 400–850 °C. The Ni(II) complex also decomposed in two steps in the temperature range 300–900 °C. The first step between 300–400 °C in the TG analysis corresponded to the elimination of two coordinated DMF molecules and the non-coordinated part of the ligand with a mass loss of 47.5 % (calcd. 47.89 %). A broad exotherm in the temperature range 200–400 °C was observed ($\Delta T_{\max} = 332.51$ °C). The second step of the decomposition was observed in the temperature range 400–900 °C with a mass loss of 42.5 % (calcd. 42.01 %). A broad exotherm in DTA could be assigned to the removal of the coordinated part of the ligand. The final weight 10 % (calcd. 9.99 %) corresponds to NiO. The TG curve of Cu(II) complex showed the first decomposition step in the temperature range 260–350 °C with a mass loss of 45.5 % (calcd. 47.60 %), and the exothermic peak on the DTA curve between 200–330 °C ($\Delta T_{\max} = 300.21$ °C) corresponds to the removal of two coordinated DMF molecules and the non-coordinated part of the ligand. The second step of the decomposition occurred in the temperature range 350–875 °C with a mass loss of 43.0 % (calcd. 41.74 %) and a broad endotherm in DTA corresponds to the removal of the coordinated part of the ligand. The final residue 11.5 % (calcd. 10.56 %) corresponds to CuO.

Antibacterial activity

The antibacterial results, Table III, showed that the ligand exhibited weak antibacterial activity but its complexes showed moderate activity against the bacteria *S. aureus* and *E. coli*. It is known that chelation tends to make the ligands act as more powerful and potent bactericidal agents, thus killing more of bacteria than the non-chelated ligand. It was observed that chelation reduces the polarity of a metal ion in a complex due to partial sharing of its positive charge with donor groups and also due to delocalization of the π electrons over whole chelate ring. Thus, chelation increases the lipophilic character in complexes and results in an enhancement of activity.³¹

TABLE III. Antibacterial and antifungal activities (Inhibition zone of bacterial growth, mm) of the ligand and its metal complexes

Compound	Antibacterial activity				Antifungal activity					
	<i>S. aureus</i>		<i>E. coli</i>		<i>A. flavus</i>	<i>C. lunata</i>		<i>P. notatum</i>		
	Concentration, mg ml ⁻¹				Concentration, µg disc ⁻¹					
	0.50	1.0	0.50	1.0	125	250	125	250	125	250
Ligand, C ₁₅ H ₁₂ O ₅	05	08	06	09	10	14	11	17	8	15
[C ₃₆ H ₃₆ N ₂ O ₁₂ Mn]	08	15	09	16	12	21	15	22	13	20
[C ₃₃ H ₂₉ NO ₁₁ ClFe]	07	12	08	15	11	19	13	19	9	19
[C ₃₆ H ₃₆ N ₂ O ₁₂ Co]	09	18	10	17	13	30	16	29	15	30
[C ₃₆ H ₃₆ N ₂ O ₁₂ Ni]	11	20	13	19	17	33	18	32	17	33
[C ₃₆ H ₃₆ N ₂ O ₁₂ Cu]	15	22	16	21	20	37	21	34	20	36
Neomycin	23	27	24	26	—	—	—	—	—	—
Griseofulvin	—	—	—	—	31	34	29	33	30	34

Antifungal activity

The antifungal results, Table III, showed that ligand exhibited moderate antifungal activity at 250 µg disc⁻¹ and its metal complexes show significant antifungal activity at the same concentration against the fungi *A. flavus*, *C. lunata* and *P. notatum*. In addition, the activity decreased as the concentration decreased. The Cu(II) complex showed greater antifungal activity than the standard at 250 µg disc⁻¹ and the Ni(II) complex showed approximately the same antifungal activity as the standard at 250 µg disc⁻¹. The order of inhibition with respect to metal ions was Cu > Ni > Co > Mn > Fe. Thus, it could be postulated that further studies of these complexes in this direction as biocides could lead to more interesting results.

The complexes are biologically active and exhibit enhanced antibacterial, antifungal activities compared to the parent ligand. The increased activity of the chelates can be explained based on the overtone concept and the Tweedy chelation theory.³² According to the overtone concept of cell permeability, the lipid membrane that surrounds the cell favours the passage of only lipid-soluble materials, for which reason liposolubility is an important factor controlling antimicrobial activity. On chelation,³³ the polarity of the metal ion was reduced greatly due to overlap of the ligand orbital and the partial sharing of its positive charge with donor groups and also due to delocalization of the π -electrons over whole chelate ring.

CONCLUSIONS

In the light of above discussion, a distorted octahedral geometry for the Cu(II) complex and an octahedral geometry for the Mn(II), Fe(III), Co(II) and Ni(II) complexes are proposed. The ligand behaves as bidentate, coordinating through the phenolic oxygen and the acetyl carbonyl group of the dehydroacetic acid moiety.

Acknowledgements. The authors are thankful to Dr. A. A. Chavan, Department of Botany, Dr. Babasaheb Ambedkar Marathwada University, Aurangabad, Maharashtra, India, for valuable suggestions.

ИЗВОД

СИНТЕЗА, СПЕКТРАЛНА, ТЕРМАЛНА И БИОЛОШКА ИСПИТИВАЊА КОМПЛЕКСА ПРЕЛАЗНИХ МЕТАЛА СА 4-ХИДРОКСИ-3-[3-(4-ХИДРОКСИФЕНИЛ)-АКРИЛОИЛ]-6-МЕТИЛ-2H-ПИРАН-2-ОНОМ КАО ЛИГАНДОМ

VAIBHAV N. PATANGE¹ и BALASAHEB R. ARBAD²

¹Department of Chemistry, Research and P. G. Center, Shri Chhatrapati Shivaji College, Omerga, Dist- Osmanabad-413606, Maharashtra и ²Department of Chemistry, Dr. Babasaheb Ambedkar Marathwada University, Aurangabad-431004, Maharashtra, India

Синтетизовани су комплекси Mn(II), Fe(III), Co(II), Ni(II) и Cu(II) са 4-хидрокси-3-[(2E)-3-(4-хидроксифенил)проп-2-еноил]-6-метил-2H-пиран-2-оном као лигандом, који је добијен из 3-ацетил-6-метил-2H-пиран-2,4(3H)-диона (дехидросирћетне киселине) и 4-хидроксибензалдехида. За карактеризацију ових комплекса употребљени су елементална микроанализа, термална, кондуктометријска, магнетна, IR, ¹H-NMR и UV-Vis мерења. Такође, испитана је антибактеријска и антифунгална активност изолованих комплекса. На основу аналитичких и спектралних података нађено је да су одговарајући јон метала и лиганд у овим комплексима координовани у 1:2 молском односу. На основу физичко-хемијских података закључено је да комплекси Cu(II) имају дисторговану октаедарску геометрију, док остали испитивани комплекси имају октаедарску геометрију. Термална анализа ових комплекса одређена је помоћу TG-DTA методе. Испитивана је *in vitro* антибактеријска активност синтетизованог лиганда и одговарајућих комплекса на грам-негативне (*Escherichia coli*) и грам-позитивне (*Staphylococcus aureus*) бактерије, као и *in vitro* антифунгална активност на сојевима *Aspergillus flavus*, *Curvularia lunata* и *Penicillium notatum*. Добијени резултати ових испитивања су показали да комплекси наведених јона метала имају већу антибактеријску/антифунгалну активност у односу на некоординовани лиганд.

(Примљено 31. маја 2010, ревидирано 4. марта 2011)

REFERENCES

1. S. S. Lim, H. S. Kim, D. U. Lee, *Bull. Korean Chem. Soc.* **28** (2007) 2495
2. M. S. Ponnurengam, S. Malliappan, K. G. Sethu, M. Doble, *Chem. Pharm. Bull.* **55** (2007) 44
3. M. L. Go, M. Liu, P. Wilairat, P. J. Rosenthal, K. L. Saliba, K. Kirk, *Antimicrob. Agents Chemother.* **48** (2004) 3241
4. L. Zhai, M. Chen, J. Blom, T. G. Theander, S. B. Christensen, A. Kharazmi, *J. Antimicrob. Chemother.* **43** (1999) 793
5. A. O. Oyedapo, V. O. Makanju, C. O. Adewunmi, E. O. Iwalewa, K. Adenowo, *Afr. J. Trad. CAM* **1** (2004) 55
6. S. J. Won, C. T. Liu, L. T. Tsao, J. R. Weng, H. H. Ko, J. P. Wang, C. N. Lin, *Eur. J. Med. Chem.* **40** (2005) 103
7. L. Miranda, J. F. Cristobal, J. F. Stevens, V. Ivanov, M. McCall, B. Feri, M. L. Deinzer, D. R. Buhler, *J. Agric. Food. Chem.* **48** (2000) 3876
8. G. S. B. Viana, M. A. M. Bandeira, F. J. A. Matos, *Phytomedicine* **10** (2003) 189
9. K. Krishanankutty, V. D. John, *Synth. React. Inorg., Met.-Org. Chem.* **28** (2003) 343

10. H. J. J. Pabon, *Recl. Trav. Chim. Pays-Bas* **83** (1964) 237
11. R. C. Srimal, B. N. Dhawan, *J. Pharm. Pharmacol.* **25** (1973) 447
12. K. K. Soudamani, R. Kuttan, *Ethnopharmacology* **27** (1989) 227
13. T. S. Rao, N. Basu, H. H. Siddique, *Indian J. Med. Res.* **75** (1982) 574
14. J. D. Lasken, A. H. Conney, *Carcinogenesis* **13** (1992) 2183
15. R. J. Anto, K. N. Dinesh Babu, R. Kuttan, *Cancer Lett.* **95** (1995) 221
16. V. N. Patange, B. R. Arbad, V. G. Mane, S. D. Salunke, *Transition Met. Chem.* **32** (2007) 944
17. V. N. Patange, B. R. Arbad, *J. Indian Chem. Soc.* **84** (2007) 1096
18. V. G. Mane, V. N. Patange, B. R. Arbad, *J. Indian Chem. Soc.* **84** (2007) 1086
19. V. N. Patange, R. K. Pardeshi, B. R. Arbad, *J. Serb. Chem. Soc.* **73** (2008) 1073
20. H. H. Thornberry, *Phytopathology* **40** (1950) 419
21. A. W. Bauer, W. M. M. Kirby, J. C. Shesies, M. Turck, *Am. J. Clin. Pathol.* **44** (1966) 93
22. N. Ramarao, V. P. Rao, V. J. Tyaga Raju, M. C. Ganorkar, *Indian J. Chem., A* **24** (1985) 877
23. O. Carugo, C. B. Castellani, M. Rizzi, *Polyhedron* **9** (1990) 2061
24. A. S. El-Tabl, T. L. Kashar, R. M. El-Bahnasawy, A. El-Monsef Ibrahim, *Pol. J. Chem.* **73** (1999) 245
25. K. Krishnankutty, M. B. Ummathur, *J. Indian Chem. Soc.* **83** (2006) 639
26. K. Nakamoto, *Infrared Spectra of Inorganic and Coordination Compounds*, Wiley Interscience, New York, 1970, pp. 159, 167, 214
27. K. A. H. Afkar, *Indian J. Chem., A* **33** (1994) 879
28. A. B. P. Lever, *Inorganic electronic spectroscopy*, Elsevier, Amsterdam, 1968
29. G. L. Eichhorn, J. C. Bailar, *J. Am. Chem. Soc.* **75** (1953) 2905
30. V. N. Patange, P. S. Mane, V. G. Mane, B. R. Arbad, *J. Indian Chem. Soc.* **85** (2008) 792
31. R. S. Shrivastava, *Inorg. Chim. Acta* **56** (1981) 165
32. N. Raman, A. Kulandaisamy, C. Tungaraja, P. Manishankar, S. Viswanthan, C. Vedhi, *Transition Met. Chem.* **29** (2004) 129
33. Z. H. Chohan, M. Arif, M. Sarfraz, *Appl. Organomet. Chem.* **21** (2007) 294.

Copyright of Journal of the Serbian Chemical Society is the property of National Library of Serbia and its content may not be copied or emailed to multiple sites or posted to a listserv without the copyright holder's express written permission. However, users may print, download, or email articles for individual use.